Enhancement of internal-noise coherence resonance by modulation of external noise in a circadian oscillator

Ming Yi,[1] Ya Jia,[2,1,*] Quan Liu,[1] Jiarong Li,[1] and Chunlian Zhu[1,3]
[1]*Department of Physics and Institute of Biophysics, Central China Normal University, Wuhan 430079, China*
[2]*CCAST (World Laboratory), P.O. Box 8730, Beijing 100080, China*
[3]*Department of Physics, Jianghan University, Wuhan 430056, China*
(Received 12 January 2006; published 24 April 2006)

A circadian oscillator driven by external noise and internal noise has been studied by use of the chemical Langevin equation method. When the system is near a Hopf bifurcation and driven by internal noise only, it is found that the coherence resonance phenomenon can be induced by the internal noise. When the system is simultaneously driven by internal and external noise, it is found that external-noise coherence resonance can be suppressed by internal noise, while internal-noise coherence resonance can be enhanced by modulation of the external noise intensity in a certain range of noise intensity. Another interesting result is that the external noise can regulate the optimal system size when the internal-noise coherence resonance occurs.

DOI: 10.1103/PhysRevE.73.041923 PACS number(s): 87.17.−d, 05.40.−a, 87.10.+e

I. INTRODUCTION

Stochastic resonance (SR) phenomena [1], which is the name coined for the rather counterintuitive fact that the response of a nonlinear system to an external periodic signal may be enhanced through an optimal amount of noise, have been intensively investigated in a large variety of physical, chemical, and biological systems [2]. However, as was shown recently, nonlinear systems with noise can also display SR-like behavior even without an external periodic signal [3–8]. This phenomenon has been called autonomous SR [3] or coherence resonance (CR) [4].

In a biochemical reaction system, it is known that the external noise and the internal noise are both unavoidable [9]. Noise in the form of random fluctuations arises in these systems in one of two ways. The external noise originates from the random variation of one or more of the externally set control parameters, such as the rate constants associated with a given set of reactions. Many previous works have demonstrated that the coherence resonance phenomenon can be induced by external noise [3–6], which is called external-noise coherence resonance (ENCR), while internal noise comes from the random fluctuations of the stochastic chemical reaction events [10] in finite-size biochemical systems. It is generally accepted that the strength of the internal noise is inversely proportional to the square root of the number of particles, an indicator of the system size V [11]. Because of their relatively small system sizes, for cellular or subcellular reaction systems, internal noise should be taken into account. The internal fluctuations can be introduced by describing the chemical reaction system as a birth-and-death stochastic process governed by a master equation [12].

Recently, there has been increasing interest in investigating the influence of internal fluctuations on various processes, such as neuron spiking [13], circadian rhythms [14–17], intracellular calcium signaling [18–20], and genetic regulation [21,22]. In finite-size biochemical systems, it has been found that internal noise can induce stochastic oscillations when the system is subthreshold or suprathreshold, the stochastic oscillations show the best performance at an optimal system size [17–22], and this phenomenon is called internal noise coherence resonance (INCR).

The largest amount of work regarding fluctuations has been focused on the consideration of systems with just one noise (either internal noise or external one). Recent work [8] has shown that the ENCR phenomenon can be induced by an external light control noise in a circadian oscillator model. It should be pointed out that the intrinsic noise of the system has not been considered there. However, for cellular or subcellular biochemical reaction systems, internal and external noise should be considered simultaneously. To our knowledge, only a few such studies have been done so far. In this paper, based on the reduced circadian oscillator model with time delay in *Drosophila* proposed by Smolen *et al.* [23], we will study the effects of both internal noise (i.e., the finite system size) and external noise (i.e., the external light control noise) on the circadian oscillating system under the suprathreshold. One of our goals is to discuss how the interplay between the externally added noise and the intrinsic noise of the system occurs.

This paper is organized as follows. In Sec. II, a mesoscopic stochastic model for the finite-size circadian oscillating system is given by virtue of the chemical Langevin equation. The effects of internal noise on the finite-size circadian oscillator without external noise have been investigated in Sec. III. In Sec. IV, taking into account the finite-size circadian oscillating system driven by an external light control noise, we will study the effects of the interplay between the externally added noise and the intrinsic noise on SNR of the circadian oscillating system. We end with conclusions in Sec. V.

II. MODEL

The model discussed in this paper is based on a two-variable model, which is a minimal representation of the

*Corresponding author. Email address: jiay@phy.ccnu.edu.cn

transcriptional regulation essential for circadian rhythm in *Drosophila* [23]. This model contains both a negative feedback loop, in which the protein *PER* binds the protein *dCLOCK* and thereby deactivates transcription of the *per* gene, and a positive feedback loop, in which activation of *per* transcription by *dCLOCK* results in binding of *dCLOCK* by *PER* and derepression of *dclock*. The reduced model consists of two differential equations, each with a time delay. The differential equations for *PER* concentration P and *dCLOCK* concentration L have two terms, one for synthesis and the other for degradation,

$$\frac{dP(t)}{dt} = v_{sp}R_{sp} - k_{dp}P(t), \tag{1}$$

$$\frac{dL(t)}{dt} = v_{sc}R_{sc} - k_{dc}L(t), \tag{2}$$

with

$$R_{sp} = \frac{L_{\text{free}}(t-\tau_1)}{K_1 + L_{\text{free}}(t-\tau_1)}, \tag{3}$$

$$R_{sc} = \frac{K_2}{K_2 + L_{\text{free}}(t-\tau_2)}, \tag{4}$$

with $L_{\text{free}}=(L-P)$ or zero, whichever is greater. The parameter values are $\tau_1=10$ h, $\tau_2=10$ h, $v_{sp}=0.5$ nM h^{-1}, $v_{sc}=0.25$ nM h^{-1}, $k_{dc}=0.5$ h^{-1}, $K_1=0.3$ nM, and $K_2=0.1$ nM. Light controls the *Drosophila* clock by triggering *PER* degradation; the first-order degradation rate constant for *PER*, k_{dp} in Eq. (1), increases with light, accordingly. Therefore, k_{dp} is a light-controlled parameter. The concentration of *PER* oscillates when $0<k_{dp}<2.8$ h^{-1}. The detailed description of the model and parameter can be found in [23].

For cellular or subcellular reaction systems, the internal noise must be considered due to the finite system size. Therefore, such a deterministic description is no longer valid; a mesoscopic stochastic model should be considered. Intuitively, one can describe such a reaction system as a birth-death stochastic process governed by a chemical master equation. Generally, there is no practical procedure to solve the chemical master equation analytically, but it still provides the basis for numerical simulation. A well-known method to handle the master equation is the high precision simulation algorithm proposed by Gillespie in 1977 [24], which mimics the reaction dynamics by randomly determining what the next reaction is and when it will happen. Though this simulation method is high precision because it accounts exactly for the stochastic nature of the reaction events, it is very time consuming and hardly applicable if the system size is large. In addition, the Gillespie algorithm takes time steps of varying length, which should be modified further in order to simulate stochastic models with time delays.

An alternative method to study the internal noise is the chemical Langevin equation (CLE) proposed by Gillespie in 2000 [25]. It is shown there that, whenever two explicit dynamical conditions are satisfied, the microphysical premise from which the chemical master equation is derived leads directly to an approximate time-evolution equation of the

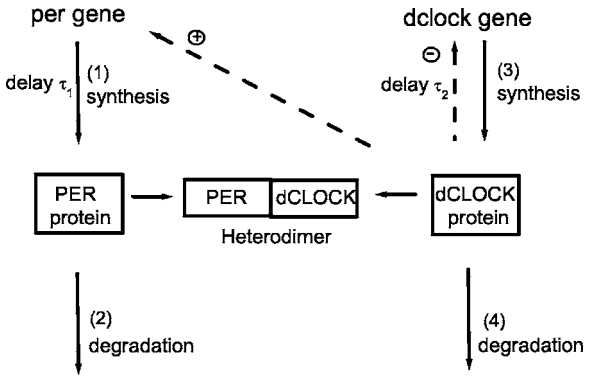

FIG. 1. Schematic of model. The *dCLOCK* protein activates the synthesis of *PER*. *PER* represses its own synthesis indirectly, by binding and inactivated *dCLOCK*. *dCLOCK* also represses its own synthesis. There are four elementary biochemical reaction processes marked with (1)–(4) respectively.

Langevin type. The CLE is a rather good approximation for the master equation if a macro-infinitesimal time scale exists and can be used to describe a system's mesoscopic dynamics. The recent works of Hou and co-workers [19–21] have shown that it is applicable to use the CLE to study the effect of the internal noise in small biochemical reaction systems qualitatively. Such a CLE clearly shows how the internal noise involved in the chemical reactions is related to the parameter values and the system size, as well as the state variables that evolve with time.

Following Gillespie's method [25], we introduce the number of *PER* protein as p and the number of *dCLOCK* protein as l. Then, the relationship between the concentration and the number of molecules is $P=p/V$ and $L=l/V$, where V is the system size. The biochemical reactions in the circadian rhythm in *Drosophila* can be grouped into four elementary processes for the current mode for a simple description of the processes as shown in Fig. 1. The corresponding transition rates for the four processes are described in Table I. Note that the transition rates $a_{j=1,\ldots,4}$ are proportional to the system size V. The two molecular species S_i $(i=1,2)$ considered here are *PER* and *dCLOCK* protein, respectively. See Table I for the four reaction channels R_j $(j=1,\ldots,4)$. The propensity function (i.e., the transition rate) a_j for R_j and the state-change vector $\vec{\nu}_j$, whose ith component ν_{ji} is the change in the number of S_i molecules produced by one R_j reaction $(j=1,\ldots,4; i=1,2)$, together completely specify the reaction channel R_j. For S_1 (i.e., *PER*), the values of ν_{ji} are $\nu_{11}=1$, $\nu_{21}=-1$, $\nu_{31}=0$, $\nu_{41}=0$; for S_2 (i.e., *dCLOCK*), the values of ν_{ji} are $\nu_{12}=0$, $\nu_{22}=0$, $\nu_{32}=1$, $\nu_{42}=-1$. Suppose the system's state at the current time t is known to be $(p(t),l(t))$. Let a random variable $K_j(p(t),l(t),\tau)$, for any $\tau>0$, be the number of R_j reactions that occur in the subsequent time interval $[t,t+\tau]$. Since each of those reactions will increase the S_i population by ν_{ji}, the number of S_i molecules in the system at time $t+\tau$ will be

$$p(t+\tau) = p(t) + K_1(p(t),l(t),\tau) - K_2(p(t),l(t),\tau), \tag{5}$$

$$l(t+\tau) = l(t) + K_3(p(t),l(t),\tau) - K_4(p(t),l(t),\tau). \tag{6}$$

An excellent approximation to $K_j(p(t),l(t),\tau)$ can be obtained if the following two conditions are imposed [25].

TABLE I. Stochastic transition processes and corresponding rates.

Transition processes	Description	Transition rates
(1) $p \to p+1$	The synthesis of *PER* activated directly by *dCLOCK* and repressed indirectly by itself	$a_1 = V v_{sp} \frac{L_{\text{free}}(t-\tau_1)}{K_1 + L_{\text{free}}(t-\tau_1)}$
(2) $p \to p-1$	The degradation of *PER*	$a_2 = V k_{dp} P(t)$
(3) $l \to l+1$	The synthesis of *dCLOCK* activated indirectly by *PER* and represented directly by itself	$a_3 = V v_{sc} \frac{K_2}{K_2 + L_{\text{free}}(t-\tau_2)}$
(4) $l \to l-1$	The degradation of *dCLOCK*	$a_4 = V k_{dc} L(t)$

Condition (i): Require τ to be small enough that the change in the state during $[t, t+\tau]$ will be so slight that none of the propensity functions changes its value appreciably. Each $K_j(p(t), l(t), \tau)$ will be a statistically independent Poisson random variable, $\mathcal{P}_j(a_j(p(t), l(t)), \tau)$. So Eqs. (5) and (6) are approximated by

$$p(t+\tau) = p(t) + \mathcal{P}_1(a_1(p(t), l(t)), \tau) - \mathcal{P}_2(a_2(p(t), l(t)), \tau), \tag{7}$$

$$l(t+\tau) = l(t) + \mathcal{P}_3(a_3(p(t), l(t)), \tau) - \mathcal{P}_4(a_4(p(t), l(t)), \tau). \tag{8}$$

Condition (ii): τ must be large enough that the expected number of occurrences of each reaction channel R_j in $[t, t+\tau]$ is much larger than 1, which allows us to approximate each Poisson random variable $\mathcal{P}_j(a_j(p(t), l(t)), \tau)$ by a normal random variable with the same mean and variance. That brings Eqs. (7) and (8) into the form

$$\begin{aligned} p(t+\tau) = p(t) &+ \mathcal{N}_1(a_1(p(t), l(t))\tau, a_1(p(t), l(t))\tau) \\ &- \mathcal{N}_2(a_2(p(t), l(t))\tau, a_2(p(t), l(t))\tau), \end{aligned} \tag{9}$$

$$\begin{aligned} l(t+\tau) = l(t) &+ \mathcal{N}_3(a_3(p(t), l(t))\tau, a_3(p(t), l(t))\tau) \\ &- \mathcal{N}_4(a_4(p(t), l(t))\tau, a_4(p(t), l(t))\tau), \end{aligned} \tag{10}$$

where $\mathcal{N}(m, \sigma^2)$ denotes the normal random variable with mean m and variance σ^2. The molecular populations from discretely changing integer variables in Eqs. (7) and (8) are converted to continuously changing real variables in Eqs. (9) and (10) in effect.

The linear combination theorem for normal random variables,

$$\mathcal{N}(m, \sigma^2) = m + \sigma \mathcal{N}(0, 1), \tag{11}$$

can now be invoked to bring Eqs. (9) and (10) into the form

$$\begin{aligned} p(t+\tau) = p(t) &+ a_1(p(t), l(t))\tau - a_2(p(t), l(t))\tau \\ &+ [a_1(p(t), l(t))\tau]^{1/2} \mathcal{N}_1(0, 1) \\ &- [a_2(p(t), l(t))\tau]^{1/2} \mathcal{N}_2(0, 1), \end{aligned} \tag{12}$$

$$\begin{aligned} l(t+\tau) = l(t) &+ a_3(p(t), l(t))\tau - a_4(p(t), l(t))\tau \\ &+ [a_3(p(t), l(t))\tau]^{1/2} \mathcal{N}_3(0, 1) \\ &- [a_4(p(t), l(t))\tau]^{1/2} \mathcal{N}_4(0, 1). \end{aligned} \tag{13}$$

First, let us regard any time interval τ that satisfies both conditions (i) and (ii) as a macroscopic infinitesimal, and denote it simply by dt. Second, let us write the "unit normal" random variable $\mathcal{N}_j(0, 1)$ as $N_j(t)$. Equations (12) and (13) become

$$\begin{aligned} p(t+\tau) = p(t) &+ a_1(p(t), l(t))dt - a_2(p(t), l(t))dt \\ &+ a_1^{1/2}(p(t), l(t)) N_1(t) (dt)^{1/2} \\ &- a_2^{1/2}(p(t), l(t)) N_2(t) (dt)^{1/2}, \end{aligned} \tag{14}$$

$$\begin{aligned} l(t+\tau) = l(t) &+ a_3(p(t), l(t))dt - a_4(p(t), l(t))dt \\ &+ a_3^{1/2}(p(t), l(t)) N_3(t) (dt)^{1/2} \\ &- a_4^{1/2}(p(t), l(t)) N_4(t) (dt)^{1/2}. \end{aligned} \tag{15}$$

Equations (14) and (15) imply the equivalent "white-noise form" Langevin equation

$$\begin{aligned} \frac{dp(t)}{dt} = &a_1(p(t), l(t)) - a_2(p(t), l(t)) + a_1^{1/2}(p(t), l(t)) \xi_1(t) \\ &- a_2^{1/2}(p(t), l(t)) \xi_2(t), \end{aligned} \tag{16}$$

$$\begin{aligned} \frac{dl(t)}{dt} = &a_3(p(t), l(t)) - a_4(p(t), l(t)) + a_3^{1/2}(p(t), l(t)) \xi_3(t) \\ &- a_4^{1/2}(p(t), l(t)) \xi_4(t), \end{aligned} \tag{17}$$

where $\xi_{i=1,\ldots,4}(t)$ are temporally uncorrelated, statistically independent Gaussian white noises with $\langle \xi_i(t) \rangle = 0$ and $\langle \xi_i(t) \xi_j(s) \rangle = \delta_{ij} \delta(t-s)$.

By using the relationship between the concentration and the molecular number, the chemical Langevin equations corresponding to the macroscopic differential equations (1) and (2) can be obtained from Eqs. (16) and (17) and read

$$\begin{aligned} \frac{dP(t)}{dt} = &[v_{sp} R_{sp} - k_{dp} P(t)] + \frac{1}{\sqrt{V}} [\sqrt{v_{sp} R_{sp}} \xi_1(t) \\ &- \sqrt{k_{dp} P(t)} \xi_2(t)], \end{aligned} \tag{18}$$

TABLE II. Reaction steps and corresponding reaction probabilities involved in the model.

Reaction step	Reaction probabilities
$p \to p+1$	$v_{sp}\Omega \dfrac{L_{\text{free}}(t-\tau_1)}{K_1\Omega + L_{\text{free}}(t-\tau_1)}\Delta t$
$p \to p-1$	$k_{dp}P(t)\Delta t$
$l \to l+1$	$v_{sc}\Omega \dfrac{K_2}{K_2\Omega + L_{\text{free}}(t-\tau_2)}\Delta t$
$l \to l-1$	$k_{dc}L(t)\Delta t$

$$\frac{dL(t)}{dt} = [v_{sc}R_{sc} - k_{dc}L(t)] + \frac{1}{\sqrt{V}}[\sqrt{v_{sc}R_{sc}}\xi_3(t) - \sqrt{k_{dc}L(t)}\xi_4(t)]. \tag{19}$$

The detailed description of the CLE method can be found in [25]. The CLEs (18) and (19) describe the effects of finite size on circadian oscillations. It can be noted that the internal noise item is proportional to $1/\sqrt{V}$ when the other parameters are fixed, so the internal noise also represents a kind of system size noise.

In fact, in order to study the intracellular biochemical reaction of finite molecules, a fixed time step algorithm has been introduced by Smolen *et al.* [23]. In contrast to the Gillespie algorithm [24], the fixed time step algorithm only requires a probabilistic determination of whether each type of chemical reaction takes place at each time step and uses a fixed time step that can be optimized to the desired accuracy. It is convenient to use this algorithm to handle some stochastic systems with time delays. Though it is an open question which algorithms are best for simulating stochastic models with time delays, this algorithm is shown to be an explicit simulation of the master equation for small time steps. In order to scale the reactions according to system size, all of the parameters sensitive to system size, e.g., v_{sp}, v_{sc}, K_1, and K_2, should be multiplied by a common factor Ω. After this rescaling, the reaction probabilities can be computed by multiplying the time step Δt with the deterministic terms in Eqs. (1) and (2) that give the rates of the specific reactions. The time step is fixed at a small enough value (5×10^{-6} h) so that the probability of each biochemical reaction is never larger than 2%. See Table II for the corresponding reaction probabilities.

In the present paper, we will use the above two methods (CLE and fixed time-step algorithm) to study the effects of internal noise on the circadian oscillator in the next section. Our numerical simulation will be exerted near the Hopf bifurcation point at about $k_{dp}^0 = 2.85\ \text{h}^{-1}$. It is a suprathreshold value at which the system is a stable steady state in the absence of noise.

III. EFFECTS OF INTERNAL NOISE ON A CIRCADIAN OSCILLATOR

In the circadian oscillator, it was already known that the external noise can induce coherence resonance and play constructive roles near the Hopf bifurcation point [8]. In this section only the internal noise is considered near the bifurcation point. Equations (18) and (19), which describe the system's dynamics with only the internal noise, can be integrated by a simple forward Euler algorithm with a time step of 0.01 h. The detailed algorithm for numerical simulation of multiplicative white noise in stochastic differential equations was given in [26].

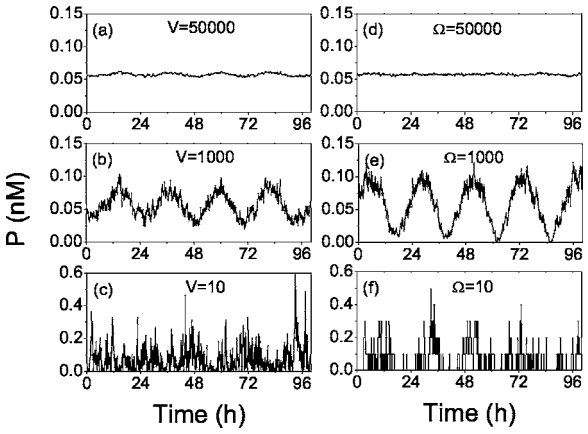

FIG. 2. Time series of *PER* concentration [(a)–(c)] via CLE and [(d)–(f)] from fixed time-step algorithm for different system size: from top to bottom $V=\Omega=5000$, 1000, and 10.

The temporal courses of *PER* concentration obtained from the CLE method [Figs. 2(a)–2(c)] and the fixed time-step algorithm [Figs. 2(d)–2(f)] are plotted in Fig. 2. For the large and small system size (i.e., the internal noise), the rhythmicity of suprathreshold circadian oscillations induced by the internal noise is inconspicuous. For the moderate system size (e.g., $V=\Omega=1000$), however, the circadian oscillations (period close to 24 h) are clearly observed. The above result shows that internal noise also can play a constructive role in such a circadian oscillator. These figures also illustrate that oscillation amplitude and variability as well as the size of fluctuations are qualitatively the same for two different simulation methods for $V=\Omega$, thus the common factor Ω in the fixed time-step algorithm corresponds to the system size V in CLE in this sense.

The effects of internal noise on the circadian oscillations can be investigated by utilizing the power spectral density PSD of proteins concentration. Figures 3(a)–3(c) plot the PSD of *PER* concentration for different system size, respectively. Clear peaks appear in the PSD. For an intermediate system size (e.g., $V=\Omega=1000$), the peak is the most pronounced among the three [see Fig. 3(b)]. The PSD curves obtained from the CLE method are almost consistent with that obtained from the fixed time-step algorithm for $V=\Omega=50000$ and 1000. From the inset of Fig. 3(c), a slight difference between two simulation methods can be seen for $V=\Omega=10$, which corresponds reasonably to the difference between Fig. 2(c) and Fig. 2(f).

To measure the relative performance of the stochastic oscillations quantitatively, we have calculated an appropriate measure β. See [3] for details about the definition and algorithm. In fact, β represents the degree of CR and is actually the signal-to-noise ratio (SNR). The dependence of β on V is

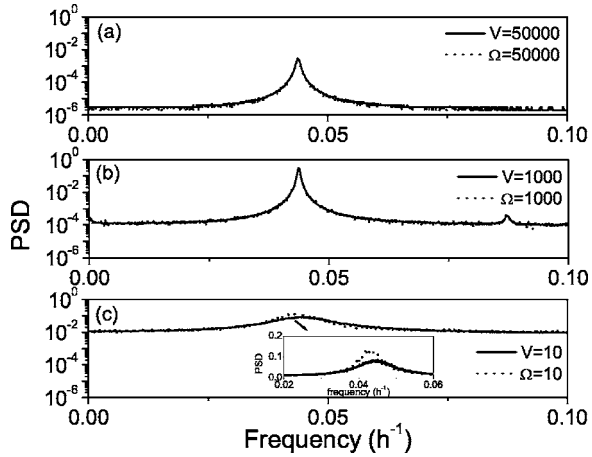

FIG. 3. The power spectral density [(a)–(c)] of *PER* concentration for different system size: from top to bottom $V=\Omega=5000$, 1000, and 10. Solid lines: data from CLE; dotted lines: data from fixed time step algorithm.

plotted in Fig. 4. A clear maximum is present for system size $V\approx 500$; an optimal system size implies an optimal level of internal noise, which demonstrates the existence of internal noise coherence resonance. Since the magnitude of the internal noise is changed via the variation of the system size, the INCR also represents a kind of system size resonance [19,22,27]. Because the PSD curves obtained from two different simulation methods are nearly the same for large system size, we will use the fixed time-step algorithm only for $V<1000$. Excellent quantitative agreement among the CLE method and the fixed time-step algorithm is apparent in the region of about $V>50$, which shows our simulation results from the CLE method are reliable in a wide range of the system size. Therefore, it is convenient to use the CLE method to study the quantitative effects of internal noise on such a mesoscopic stochastic model.

IV. EFFECTS OF BOTH INTERNAL AND EXTERNAL NOISE ON A CIRCADIAN OSCILLATOR

The effects of only external noise on the circadian oscillator have been investigated in Ref. [8], where the external noise is introduced through the light-controlled parameter k_{dp} in Eq. (1). The effects of both internal and external noise on a circadian oscillator will be investigated in this section.

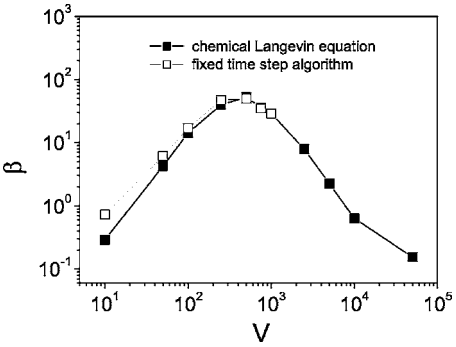

FIG. 4. Dependence of the measure of coherence (β) on the system size for $k_{dp}^0=2.85$ h^{-1}. Solid squres: results obtained via CLE; open squares: results from fixed time-step algorithm for $V<1000$.

Consider that (i) the internal noise and the external noise are independent of each other. The last two noise terms in CLEs (18) and (19) are multiplicative, which only describe the intrinsic noise of the finite-size system due to the random biochemical reaction processes. (ii) Although the external light-controlled parameter k_{dp} appeared in both the second term and the last term in Eq. (18), respectively, the second term, $k_{dp}P(t)$, determines the kinetic properties of the biochemical system, while the role of the last term, $\sqrt{k_{dp}P(t)}\xi_2(t)/\sqrt{V}$, in the evolution of the system is much more smaller than that of the second term, especially in the case of large system size (i.e., $V\gg 1$). For simplicity, here the external noise is only introduced through the light-controlled parameter k_{dp} in the second term in CLE (18), and takes the form of

$$k_{dp}=k_{dp}^0[1+\eta(t)], \tag{20}$$

where $\eta(t)$ is Gaussian white noise with zero mean, and its autocorrelation function is $\langle\eta(t)\eta(t')\rangle=2D\delta(t-t')$; D is the light noise intensity. The light-controlled parameter k_{dp} in the last term in CLE (18) is taken by the constant k_{dp}^0, and its fluctuation is neglected in the present paper. Therefore, the CLEs (18) and (19) become

$$\frac{dP(t)}{dt}=[v_{sp}R_{sp}-k_{dp}^0[1+\eta(t)]P(t)]+\frac{1}{\sqrt{V}}[\sqrt{v_{sp}R_{sp}}\xi_1(t)-\sqrt{k_{dp}^0P(t)}\xi_2(t)], \tag{21}$$

$$\frac{dL(t)}{dt}=[v_{sc}R_{sc}-k_{dc}L(t)]+\frac{1}{\sqrt{V}}[\sqrt{v_{sc}R_{sc}}\xi_3(t)-\sqrt{k_{dc}L(t)}\xi_4(t)]. \tag{22}$$

Equations (21) and (22) describe the circadian oscillator driven by both the internal noise and the external noise under the approximation that the coupling between them is ignored.

In order to give a simple and clear analysis about the interplay between the external noise and the intrinsic noise of the system near the bifurcation point, we have investigated how the coherence resonance phenomenon induced by one noise is affected by the other noise.

First, we have investigated how the external-noise coherence resonance is affected by the internal noise. The dependence of β on the external-noise intensity for different choices of system size is plotted in Fig. 5. When the system size is large (e.g., $V=100\,000$), the dependence is obviously close to our previous result without the internal noise, showing the occurrence of the external-noise coherence resonance. With the decrease of system size, the ENCR curve becomes lower. Once the system size drops to $V=250$, it is found that β monotonically decreases slightly with the increment of D and the peak disappears. Now, because the system size becomes very small, the internal noise becomes strong enough to make the total noise only play a destructive role.

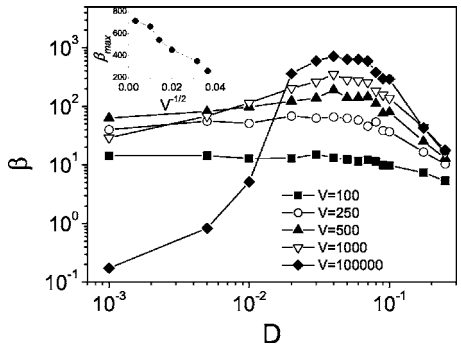

FIG. 5. The external-noise coherence resonance for different system size. Inset: β_{max} of ENCR vs $1/\sqrt{V}$.

Furthermore, the internal noise strongly dominates the stochastic behavior at $V=100$, which causes β nearly to remain unchange with D.

In [28], a quantity of SNR_{max} was used to study the role of spatially correlated stochastic perturbations on a neural network. In order to grasp the most important information provided in Fig. 5, we also choose the maximum SNR value (β_{max}) from each ENCR curve and plot the dependence of β_{max} on $1/\sqrt{V}$ (see the inset graph in Fig. 5). Since $1/\sqrt{V}$ measures the internal-noise intensity, it is shown that β_{max} decreases with the increase of the internal noise. This result implies that internal noise can suppress ENCR in the circadian oscillator.

Secondly, we have investigated how the internal noise coherence resonance is affected by the external-noise. The dependence of β on the system size for different choices of external-noise intensity is shown in Fig. 6. At $V=10$, the internal noise is so large that the system is insensitive to the change of external noise. Therefore, these values of β for different D are almost the same. While the internal noise is very small at $V=100\,000$, β increases at first and then declines with increasing of D, which reasonably illustrates the occurrence of external-noise coherence resonance. After $V=100\,000$, the internal noise can nearly be neglected and a plateau will form on each curve naturally.

When the external noise is very small (e.g., $D=0.001$), the dependence of β is close to the result shown in Fig. 4. The internal-noise coherence resonance occurs only for $D<0.04$; in such a region of D, the INCR curve becomes

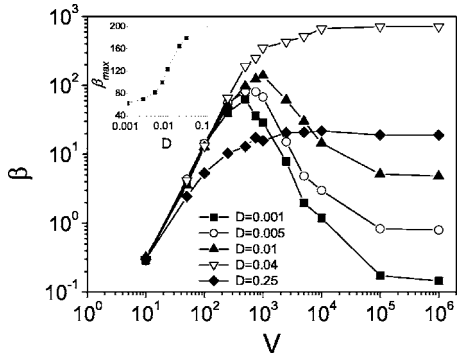

FIG. 6. The internal noise coherence resonance of different external-noise intensity. Inset: β_{max} of INCR vs D.

higher as the external noise increases. If $D \geqslant 0.04$, β monotonically increases at first, and then reaches a plateau directly; the peak disappears. It is because the external noise becomes so large that the total noise can only play a destructive role. When D increases further, the plateau on the curve becomes lower. We choose β_{max} only from each INCR curve. From the inset graph in Fig. 6, β_{max} raises with the increment of external noise, which shows the external noise can enhance INCR in the range of $0<D<0.04$. Since SNR is the ratio of the amplitude of the desired signal to the amplitude of noise signals, the phenomenon of external-noise-enhanced INCR also reveals that the internal noise is suppressed by the external noise through increasing the maximum SNR of INCR, which displays another constructive role of external noise [29]. In studying CR, different clues to enhance the strength of it have been found, such as noise delay [30], the couplings of elements [31], and the distance to the bifurcation point [32]. Here, a clue to enhance the strength of INCR is the modulation of the external-noise intensity in a certain range. Though it is not easy for us to directly control the external noise intensity to obtain the maximum SNR, we expect that biological systems may use the above regulatory mechanism to play functional roles in cellular process.

In addition, an interesting result is that the optimal system size is controlled by the external noise when the INCR occurs. It is found that the optimal system size changes from about 500 to 1000 in Fig. 6. In the above region of system size, our simulation result via CLE is rather reliable (see Fig. 4). It is also interesting to note that the optimal system size is comparable to that obtained in [19]. The biological organism may adapt to adjust the optimal size according to the external noise. As a useful extension of the previous work about system size resonance [17,20], this result will help us to understand the activity of biological systems better.

In order to understand the above effects of the interplay between the externally added noise and the intrinsic noise on SNR of the circadian oscillating system, we will analyze the mechanisms of noise control in the stochastic dynamics of coherence resonance. It is known that different noise sources may affect the system's stochastic dynamics in different ways [32,33]. Here, the external noise term is added directly to the deterministic equation multiplicatively, while the internal noise introduced in the chemical reactions is related to the parameter values and the system size, as well as the state variables that evolve with time. Therefore, the mechanisms of the coherence resonance phenomenon induced by internal and external noise, respectively, may be different. The maximum of SNR is about 50 when only internal noise exists (see Fig. 4), but about 700 when only external noise exists [8]. Thus, the optimizing performance of stochastic oscillations by the external noise is much more than that by the internal noise. When the internal noise coherence resonance occurs, the added external noise can enhance the performance of stochastic oscillations by introducing extra dynamics. The extra dynamics may play a crucial role as an energy source, which makes β_{max} increase with increasing D, until the total noise loses its constructive role (see Fig. 6). On the contrary, when the external-noise coherence resonance occurs, the added internal noise only can reduce the performance of stochastic oscillations, which makes β_{max} decrease with de-

creasing V (see Fig. 5). In [33], the generation of doubly stochastic coherence due to two noise sources in bistable neural models is investigated analytically, which will motivate us to make a clearer study about the present results in the future.

V. CONCLUSIONS

In conclusion, we have constructed a mesoscopic stochastic model for a circadian oscillator. When the system is near a Hopf bifurcation and driven by the internal noise only, the existence of internal-noise coherence resonance is found. In contrast to the analysis done previously, we have taken into account a combination of internal and external noise. It is found that external-noise coherence resonance can be suppressed by internal noise, while internal-noise coherence resonance can be enhanced by modulation of the external-noise intensity in a certain range of noise intensity. The external-noise-enhanced INCR also reveals that the external noise can suppress the internal noise through increasing the SNR of INCR. A preliminary analysis about the interplay between the externally added noise and the intrinsic noise on SNR of the circadian oscillating system is given. Another interesting result is that the optimal system size can be regulated by the external noise when the internal-noise coherence resonance occurs.

The above results would be helpful to understand how the interplay between the internal and external noises in the circadian oscillator is involved in the mechanisms for coherence resonance, although it is not still clear whether biological systems use the above regulatory mechanism to play functional roles in cellular process.

It should be pointed out that the above results about the effects of external noise and internal noise together on the circadian oscillator are just obtained from Eqs. (21) and (22), that is, the external noise and the intrinsic noise considered here are independently introduced in the mesoscopic stochastic model after our approximate treatment. Indeed, when the system size or the number of reactant molecules is very small, the interaction between the internal and external noise would be very strong and important. The study of the coupling effects of internal and external noise [i.e., the interaction between the internal and external noise appearing in the last term of Eq. (21)] on stochastic dynamics is our further work. We expect that more novel and richer physical phenomena will be observed when the system size is small enough and the coupling between two kinds of noise should be considered.

ACKNOWLEDGMENTS

This work was supported by the National Natural Science Foundation of China under Grants No. 10575041 (Y.J.) and No. 90303007 (J.R.L), and partly by MOE of China under project SRFDP-20040511005 (Y.J.).

[1] R. Benzi, A. Sutera, and A. Vulpiani, J. Phys. A **14**, L453 (1981); R. Benzi, G. Parisi, A. Sutera, and A. Vulpiani, Tellus **34**, 10 (1982); C. Nicolis, *ibid.* **34**, 1 (1982).

[2] K. Wiesenfeld and F. Moss, Nature (London) **373**, 33 (1995); A. Förster, M. Merget, and F. W. Schneider, J. Phys. Chem. **100**, 4442 (1996); L. Gammaitoni, P. Hänggi, P. Jung, and F. Marchesoni, Rev. Mod. Phys. **70**, 223 (1996); A. Guderian, G. Dechert, K. Zeyer, and F. Schneider, J. Phys. Chem. **100**, 4437 (1996); Y. Jia, S. N. Yu, and J. R. Li, Phys. Rev. E **62**, 1869 (2000); Y. Jia, X. P. Zheng, X. M. Hu, and J. R. Li, *ibid.* **63**, 031107 (2001).

[3] G. Hu, T. Ditzinger, C. Z. Ning, and H. Haken, Phys. Rev. Lett. **71**, 807 (1993).

[4] A. S. Pikovsky and J. Kurths, Phys. Rev. Lett. **78**, 775 (1997).

[5] A. Longtin, Phys. Rev. E **55**, 868 (1997).

[6] A. Neiman, P. I. Saparin, and L. Stone, Phys. Rev. E **56**, 270 (1997).

[7] P. Hänggi, ChemPhysChem **3**, 285 (2002).

[8] M. Yi and Y. Jia, Phys. Rev. E **72**, 012902 (2005).

[9] Y. Harada, T. Funatsu, K. Murakami, Y. Nonoyama, A. Ishihama, and T. Yarnagida, Biophys. J. **76**, 709 (1999); J. Hasty, J. Pradines, M. Dolnik, and, J. J Collins, Proc. Natl. Acad. Sci. U.S.A. **97**, 2075 (2000); P. S. Swain, M. B. Elowitz, and E. D. Siggia, *ibid.* **99**, 12795 (2002).

[10] H. H. McAdams and A. Arkin, Proc. Natl. Acad. Sci. U.S.A. **94**, 814 (1997); A. P. Arkin, J. Ross, and H. H. McAdams, Genetics **149**, 1633 (1998); N. Barkai and S. Leibler, Nature (London) **403**, 267 (1999); C. V. Rao, D. M. Wolf, and A. Arkin, Nature (London) **420**, 231 (2002).

[11] E. Schrödinger, *What is Life?: With Mind and Matter and Autobiographical Sketches* (Cambridge University Press, Cambridge, U K, 1992).

[12] N. G. Van Kampen, *Stochastic Processes in Physics and Chemistry* (North-Holland, Amsterdam, 1981).

[13] M. S. Wang, Z. H. Hou, and H. W. Xin, ChemPhysChem **5**, 1602 (2004).

[14] A. Becskei, B. Séraphin, and L. Serrano, EMBO J. **20**, 2528 (2001).

[15] J. M. Vilar, H. Y. Kueh, N. Barkai, and S. Leibler, Proc. Natl. Acad. Sci. U.S.A. **99**, 5988 (2002).

[16] D. Gonze, J. Halloy, and P. Gaspard, J. Chem. Phys. **116**, 10997 (2002); D. Gonze, J. Halloy, and A. Goldbeter, Proc. Natl. Acad. Sci. U.S.A. **99**, 673 (2002).

[17] Z. H. Hou and H. W. Xin, J. Chem. Phys. **119**, 11508 (2003).

[18] J. W. Shuai and P. Jung, Phys. Rev. Lett. **88**, 068102 (2002).

[19] H. Y. Li, Z. H. Hou, and H. W. Xin, Chem. Phys. Lett. **402**, 444 (2005).

[20] H. Y. Li, Z. H. Hou, and H. W. Xin, Phys. Rev. E **71**, 061916 (2005).

[21] Z. W. Wang, Z. H. Hou, and H. W. Xin, Chem. Phys. Lett. **401**, 307 (2005).

[22] R. Steuer, C. S. Zhou, and J. Kurths, BioSystems **72**, 241 (2003).

[23] P. Smolen, D. A. Baxter, and J. H. Byrne, Biophys. J. **83**, 2349

(2002).
[24] D. T. Gillespie, J. Phys. Chem. **81**, 2340 (1977).
[25] D. T. Gillespie, J. Chem. Phys. **113**, 297 (2000).
[26] J. M. Sancho, M. San Miguel, S. L. Katz, and J. D. Gunton, Phys. Rev. A **26**, 1589 (1982).
[27] B. von Haeften, G. Izús, and H. S. Wio, Phys. Rev. E **72**, 021101 (2005).
[28] N. Montejo, M. N. Lorenzo, V. Pérez-Villar, and V. Pérez-Muñuzuri, Phys. Rev. E **72**, 011902 (2005).
[29] J. M. G. Vilar and J. M. Rubi, Phys. Rev. Lett. **86**, 950 (2001).
[30] Z. H. Hou and H. W. Xin, Phys. Lett. A **263**, 360 (1999).
[31] Y. Shinohara, T. Kanamaru, H. Suzuki, T. Horita, and K. Aihara, Phys. Rev. E **65**, 051906 (2002).
[32] Y. P. Li and Q. S. Li, J. Chem. Phys. **120**, 8748 (2004).
[33] A. Zaikin, J. Garcia-Ojalvo, R. Báscones, E. Ullner, and J. Kurths, Phys. Rev. Lett. **90**, 030601 (2003).